An Economical Class of Droop-Compensated Generalized Comb Filters: Analysis and Design

G. Jovanovic Dolecek, *Senior Member, IEEE*, and Massimiliano Laddomada, *Senior Member, IEEE*

***Abstract*—In this brief, we address the design of economical recursive generalized comb filters (GCFs) by proposing an efficient technique to quantize the multipliers in the z-transfer function employing power-of-2 (PO2) terms. GCFs are efficient anti-aliasing decimation filters with improved selectivity and quantization noise rejection performance around the so-called folding bands with respect to classical comb filters. The proposed quantization technique guarantees perfect pole–zero cancelation in the rational z-transfer function of the GCFs, thus totally avoiding instability problems. Moreover, we propose the use of a simple droop compensator for the sake of recovering the passband droop distorting the useful digital signal in the baseband. A design example is proposed with the aim of showing the application of the proposed technique, and a practical architecture of a sample third-order GCF is discussed.**

***Index Terms*—Cascaded integrator-comb (CIC) filters, comb, decimation, decimation filter, delta-sigma, generalized comb filter (GCF), power-of-2 (PO2), sinc filters.**

I. Introduction and Problem Formulation

THE DESIGN of computationally efficient decimation filters for $\Sigma\Delta$ analog-to-digital (A/D) converters, as well as general multistage decimation architectures, is a well-known research topic [1]–[4].

To define the notation employed throughout this brief, consider an analog signal $x(t)$ (with bandwidth $[-B_x, +B_x]$) analog-to-digitally sampled with a frequency $f_s = 1/T_s$, which is hereafter called sampling frequency. Let $f_s = \rho \cdot 2B_x$. With this setup, the normalized digital bandwidth of the discrete-time signal $x(nT_s)$ can be written as $[-(B_x/f_s), +(B_x/f_s)] = [-(1/2\rho), +(1/2\rho)]$.

For ease of notation, let $f_o = 1/2\rho$. We notice in passing that $\rho = 1$ corresponds to sampling a signal at the Nyquist frequency, and no oversampling is accomplished on the analog signal $x(t)$. On the other hand, for $\rho \gg 1$, we are dealing with oversampled A/D converters, and the sampled signal $x(nT_s)$ has to be decimated down to the Nyquist frequency to be processed by digital signal processing algorithms.

Oversampled digital signals are practically decimated down to the so-called Nyquist frequency using a cascade of two (or more) decimation stages, as suggested by Crochiere and Rabiner in the landmark paper [5] (see also [7]), and the frequency response $H(e^{j\omega})$ of the first decimation filter in the cascade must attain the design specifications in the frequency ranges (hereafter called folding bands) defined as $[(k/D) - f_c; (k/D) + f_c]$, with $k = 1, \ldots, \lfloor (D/2) \rfloor$. The reason lies in the observation that the spectral content falling inside these frequency bands will fold down to baseband because of the sampling rate reduction by D in the first decimation stage, hence inevitably affecting the signal resolution after the multistage decimation chain [7]. Unlike classical finite-impulse response (FIR) filters designed to meet predefined specifications over the whole digital frequency axis $[0, +1/2]$, decimation filters must be designed to meet proper specifications only in the folding bands [5], [7].

In a multistage decimation architecture, the first decimation stage usually exploits N cascaded stages with an overall z-transfer function defined as [2]

$$H_{C_N}(z) = \left(\frac{1}{D}\frac{1-z^{-D}}{1-z^{-1}}\right)^N = \frac{1}{D^N}\prod_{i=1}^{D-1}\left(1 - z^{-1}e^{j\frac{2\pi}{D}i}\right)^N \tag{1}$$

where D is the desired decimation factor. Its main advantage over other filters stems from the following facts: 1) It presents an inherent anti-aliasing effect since its zeros fall in the folding bands $[(k/D) - f_c; (k/D) + f_c]$, with $k = 1, \ldots, \lfloor (D/2) \rfloor$. 2) It is extremely simple to implement. 3) It does not require any multiplier in the practical architecture. However, the magnitude response exhibits a considerable passband droop, which, in turn, deteriorates the downsampled signal.

Generalized comb filters (GCFs) were introduced in [8] with the goal of improving the selectivity performance of classical comb filters around the folding bands previously defined. As an instance, compared to a classical third-order comb filter [$H_{C_N}(z)$ in (1) with $N = 3$], a third-order GCF has z-transfer function

$$H_3(z) = H_0\frac{1-z^{-D}}{1-z^{-1}}\frac{1-z^{-D}e^{-j\alpha D}}{1-z^{-1}e^{-j\alpha}}\frac{1-z^{-D}e^{j\alpha D}}{1-z^{-1}e^{j\alpha}} \tag{2}$$

whereby α is defined as [8]

$$\alpha = q2\pi f_o. \tag{3}$$

Basically, α applies a rotation to the zeros of a classical comb filter by spreading them across the folding bands. Indeed, choosing $0 \leq q \leq 1$, the rotated zeros fall in the folding bands. (Notice that GCFs become classical comb filters by choosing $q = 0 \Rightarrow \alpha = 0$; in this respect, GCFs generalize classical comb filters.) The main drawback of GCFs lies on the presence of real coefficients due to the applied zero rotation.

Manuscript received September 14, 2009; revised November 20, 2009. Current version published April 21, 2010. This paper was recommended by Associate Editor P. Kumar Meher.

G. J. Dolecek is with the Department of Electronics, Institute INAOE, 72000 Puebla, Mexico (e-mail: gordana@inaoep.mx).

M. Laddomada is with the Department of Electrical Engineering, Texas A&M University, Texarkana, TX 75505 USA (e-mail: mladdomada@tamut.edu).

Digital Object Identifier 10.1109/TCSII.2010.2043469

With this background, let us provide a quick survey of the recent literature related to the problem addressed here.

A third-order modified decimation sinc filter was proposed in [9] and still further analyzed in [10] and [11]. Other works somewhat related to the topic addressed in this brief are [12]–[22]. Gao *et al.* [12] and Aboushady *et al.* [13] proposed computational efficient decimation filter architectures for implementing classical comb filters. Kwentus *et al.* [14] proposed the use of decimation sharpened filters embedding comb filters, whereas Dolecek and Mitra [15] addressed the design of a novel two-stage sharpened comb decimator. Laddomada and Mondin [20] and Daneshgaran and Laddomada [21] proposed novel decimation schemes for $\Sigma\Delta$ A/D converters based on Kaiser and Hamming sharpened filters and then generalized in [22] for higher order decimation filters. Laddomada [16] proposed the design of multistage decimation architectures relying on constituent cyclotomic polynomial filters. Dolecek and Mitra [17] proposed compensation filters to decrease the passband droop of classical comb filters. This work was then extended in [18] and [19].

The main aim of this brief is to propose a recursive droop-compensated multiplierless architecture for implementing the GCFs proposed in [8]. To this end, in Section II, we briefly recall the z-transfer function of third-order GCFs and highlight their main peculiarities with respect to classical comb filters. Then, we present the technique to quantize the multipliers in order to meet perfect pole–zero cancelation. In Section III, we present a sample design example, as well as an effective architecture for implementing recursive multiplierless GCFs. In Section IV, we present a simple second-order droop compensator to recover the passband distortion introduced by this class of decimation filters. The design of higher order GCFs is briefly addressed in Section V, whereas Section VI draws the conclusion.

II. Design of Economical Third-Order GCFs

This section presents the details of the technique proposed for designing multiplierless recursive GCFs. To get started, let us introduce the z-transfer function of a third-order GCF

$$H_3(z) = H_0 \frac{1-z^{-D}}{1-z^{-1}} \frac{1-2\cos(\alpha D)z^{-D}+z^{-2D}}{1-2\cos(\alpha)z^{-1}+z^{-2}} \quad (4)$$

where H_0 is a constant term ensuring unity baseband gain.[1] We notice in passing that higher order GCFs can straightforwardly be designed by applying the technique presented in this section for replacing the real coefficients with power-of-2 (PO2) terms, as briefly explained in Section V.

To move forward, consider the two multipliers in the z-transfer function (4)

$$a = 2\cos(\alpha D) \quad (5)$$

$$b = 2\cos(\alpha). \quad (6)$$

To present the key idea of this section, let us discuss some specific examples. First, consider the case $D = 2$. Upon using known formulas from trigonometry [23], the multiplier a can be rewritten as

$$\begin{aligned} a &= 2\cos(\alpha D) = 2\left[2\cos^2(\alpha) - 1\right] \\ &= 4\cos^2(\alpha) - 2. \end{aligned} \quad (7)$$

The key idea is that both multipliers a and b can be expressed as a function of the common term $\cos(\alpha)$. Hence, upon quantizing $\cos(\alpha)$, exact pole–zero cancelation is guaranteed, and the filter $H_3(z)$ does not suffer from instability problems. A useful approximation is the one that represents $\cos(\alpha)$ as PO2 coefficients. By doing so, the multipliers are realized as shifters, which turn to be an economical solution as long as the practical implementation of these filters is concerned.

This idea can easily be extended to any desired decimation factor D recalling the relation [23]

$$\cos(\alpha D) = 2\cos\left(\alpha(D-1)\right)\cos(\alpha) - \cos\left(\alpha(D-2)\right). \quad (8)$$

As an instance, consider $D = 3$. Upon using (8), the first multiplier can be rewritten as a function of $\cos(\alpha)$ as follows:

$$\begin{aligned} a &= 2\cos(3\alpha) = 4\cos(2\alpha)\cos(\alpha) - 2\cos(\alpha) \\ &= 8\cos^3(\alpha) - 6\cos(\alpha). \end{aligned} \quad (9)$$

For $D = 4$, the first multiplier can be rewritten as a function of $\cos(\alpha)$ using the following relation:

$$a = 2\cos(4\alpha) = 16\cos^4(\alpha) - 16\cos^2(\alpha) + 2. \quad (10)$$

On the same line, for $D = 8$, it is

$$\begin{aligned} a &= 2\cos(8\alpha) \\ &= 256\cos^8(\alpha) - 512\cos^6(\alpha) \\ &\quad + 320\cos^4(\alpha) - 64\cos^2(\alpha) + 2. \end{aligned} \quad (11)$$

A. Recursive Multiplierless Design of GCFs

In order to find a PO2 expansion of the multipliers a and b, we quantize $\cos(\alpha)$ as follows:

$$\cos(\alpha) = 2^{-k} I \quad (12)$$

where I, which is a proper integer, can be represented as a sum of PO2 terms as well.

The next line of pursuit consists of finding the best integer k to represent $\cos(\alpha)$ in (12).

Upon noting that $\cos(\alpha) \leq 1\ \forall\alpha$, we obtain

$$\cos(\alpha) = 2^{-k} I \quad I_{\max} = 2^k - 1. \quad (13)$$

Therefore, it is

$$\cos(\alpha) \leq 2^{-k}(2^k - 1) = 1 - 2^{-k}. \quad (14)$$

Upon solving (14) for k, the following inequality easily follows:

$$k \geq -\log_{10}\left(1 - \cos(\alpha)\right) / \log_{10} 2. \quad (15)$$

[1] Notice that, being a constant scaling factor, H_0 is irrelevant to the analysis developed henceforth.

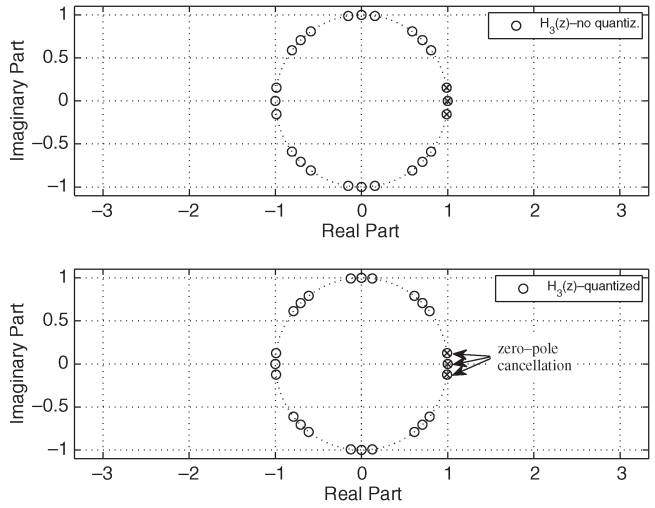

Fig. 1. Zero–pole diagram related to the filter $H_3(z)$ employing (upper subplot) real coefficients a and b and (lower subplot) quantized multipliers. The zeros are denoted by circles, and the poles are denoted by crosses.

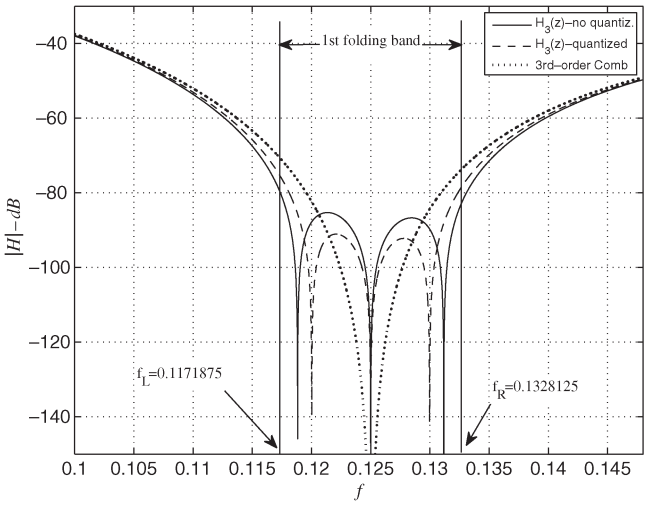

Fig. 2. Frequency responses of $H_3(z)$ employing real (Label $H_3(z)$-no quantiz.) and quantized (Label $H_3(z)$-quantized)coefficients, compared with the frequency response of a third-order comb filter in the first folding band falling in the frequency interval [0.1171875, 0.1328125]. Notice the improved zero displacement of the proposed filters within the folding band, compared to the behavior of a classical comb filter: this is the reason $H_3(z)$ guarantees improved quantization noise rejection relative to an equivalent-order comb filter (of third order in this specific example).

This relation can be used to find the least integer value of k for representing $\cos(\alpha)$ as $\cos(\alpha) = 2^{-k}I$ while $I = 2^k - 1$.

This technique is applied in the next section to a specific design example.

III. Design Example

This section presents a sample design example in order to highlight the design steps for choosing the parameters appearing in the proposed decimation filters. Comparisons are also provided with respect to classical comb filters, as well as with GCFs without multiplier quantization.

In this design example, we consider a decimation factor $D = 8$ and an oversampling factor $\rho = 64$. This setup identifies a two-stage decimation architecture whereby the first stage embeds the anti-aliasing filter proposed in this work with $D = 8$ whereas the second stage decimates by 8. We notice in passing that the second stage may employ the same GCF or any classical decimation filter, such as comb filters.

The normalized bandwidth of the sampled signal is $f_o = 1/2\rho = 0.0078125$ (this means that the analog bandwidth B_x is mapped to the digital frequency interval $[-f_o, +f_o]$ after A/D conversion with sample rate f_s), whereas the first folding band is located in the interval

$$\left[\frac{1}{D} - f_o; \frac{1}{D} + f_o\right] = [0.1171875; 0.1328125]\,.$$

Considering $\alpha = q2\pi f_o = 0.038779$ ($q = 0.79$ is the optimal zero rotation derived in [8]), from (15), the values $k = 11$ and $I_{\max} = 2047$ easily follow.

The zero–pole diagram of the proposed filter $H_3(z)$ employing real coefficients ($a = 1.904525373682791$ and $b = 1.998496374942524$) is depicted in the upper subplot of Fig. 1, whereas the lower subplot shows the zero–pole diagram for the same filter employing the quantized multipliers $a = 1.937819809321525$ obtained using (11) and (13) with the values $k = 11$ and $I_{\max} = 2047$, and $b = 2^{-k+1}I_{\max} = 1.9990234375$. The key observation from Fig. 1 is the perfect zero–pole cancelation guaranteed by the filter $H_3(z)$ with quantized coefficients. Moreover, notice that the quantization of poles and zeros does not move the roots outside the unit circle in the z-plane. The only effect is a slight displacement over the unit circle, compared to the roots of the filter employing real coefficients. Moreover, a quick comparison between the two subplots of Fig. 1 shows that the zero–pole locations of both filters are fairly similar, thus confirming the effectiveness of the proposed quantization framework for avoiding real coefficients and allowing stable recursive implementation of the proposed filters. This also implies that the noise rejection performance of the quantized filter $H_3(z)$ is the same as that of the filter embedding real coefficients. Better insights in the zero locations within the first folding band can be gained by the plot shown in Fig. 2, where the frequency responses of $H_3(z)$ employing real and quantized coefficients are compared with the frequency response of a third-order comb filter. Notice the presence of the rotated zeros spanning the first folding band $[(1/8) - 0.0078125; (1/8) + 0.0078125]$.

An effective architecture for implementing the proposed third-order filters is shown in Fig. 3. Such architecture can be obtained by expanding the polynomials at the numerator and denominator in (4). Developing the cross terms in (4), setting $m = 1 + b$ and $n = 1 + a$, and neglecting the scaling factor H_0, the following z-transfer function can easily be obtained:

$$H_3(z) = \frac{1 - n(z^{-D} - z^{-2D}) - z^{-3D}}{1 - m(z^{-1} - z^{-2}) - z^{-3}}. \qquad (16)$$

Some considerations are in order. Using well-known noble multirate identities [4], the polynomial $1 - n(z^{-D} - z^{-2D}) - z^{-3D}$ at the numerator becomes $1 - n(z^{-1} - z^{-2}) - z^{-3}$ when moved after the decimator by D block. The recursive part of the filter $1/(1 - m(z^{-1} - z^{-2}) - z^{-3})$ is realized in front of the decimator block. We notice in passing that the delays in the left side of the decimator by D operate at a rate D times higher

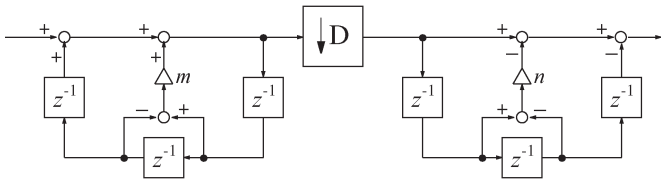

Fig. 3. Recursive implementation of the decimation filter $H_3(z)$. The coefficients in the figure are $m = 1 + b$ and $n = 1 + a$.

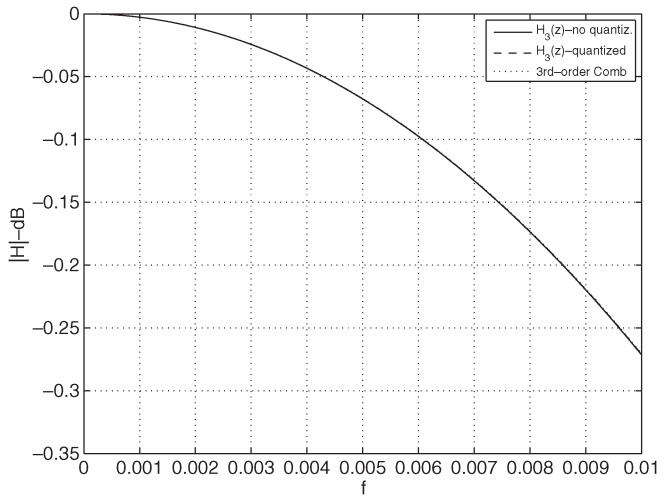

Fig. 4. Passband behaviors of the investigated filters in the frequency range [0, 0.01]. The curve labeled $H_3(z)$-*quantized* refers to the proposed filter with quantized coefficients, whereas the curve $H_3(z)$-*no quant.* refers to the same filter employing real coefficients. Finally, the curve labeled *3-rd order Comb* refers to a third-order comb filter. Notice that the three frequency responses are superimposed. Notice that the worst case passband distortion occurs at the normalized signal frequency $f_o = 0 : 0078125$.

than the ones on the right side [24], even though, for simplicity, we did not specify it.

Fig. 4 shows that the passband behavior of the proposed GCFs, regardless of multiplier quantization, is very similar to that of a classical third-order comb filter. Because of the passband droop introduced, the latter class of filters can be used to decimate the signal down to four times the Nyquist frequency [3], thus limiting their applicability in multistage architectures. So is for the GCFs presented in this brief. In addition, a FIR filter is usually employed at the end of the multistage architecture for the sake of recovering such signal distortion. For the sake of counteracting the signal distortion issue, the next section proposes the use of a droop compensator.

IV. Droop Compensation of GCFs

The passband droop of GCFs is similar to that imposed by equivalent-order classical comb filters. For the sake of compensating this distortion, we employ the multiplierless compensator proposed in [17].

The z-transfer function of this droop compensator is

$$H_c(z) = A\left[1 + Bz^{-D} + z^{-2D}\right] \tag{17}$$

where $A = -2^{-(r+1)}$, $B = -(2^{r+2} + 2)$, and r is a proper design parameter noted in Table I. Notice that the z-transfer function $H_c(z)$ becomes the second-order polynomial $A[1 + Bz^{-1} + z^{-2}]$ when moved after the decimator by D.

TABLE I
Optimal Parameter r of the GCF Droop Compensator

GCF order	2	3	4	5	6
r	2	2	1	0	0

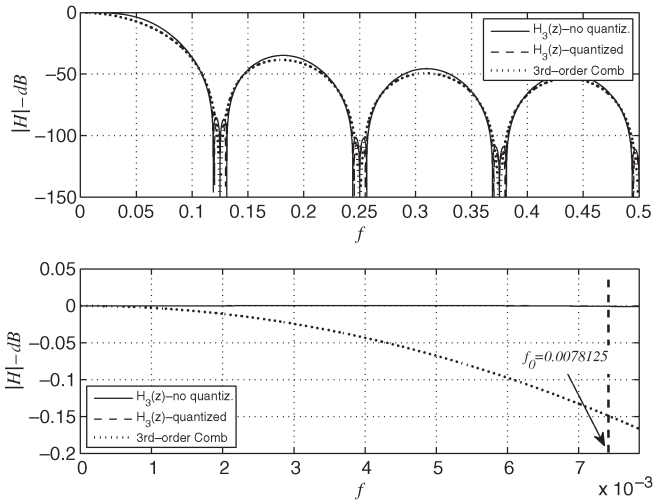

Fig. 5. (Upper subplot) Frequency responses of $H_3(z)$ employing real (Label $H_3(z)$-no quantiz.) and quantized (Label $H_3(z)$-quantized) coefficients and droop compensator, compared with the frequency response of a third-order comb filter. (Lower subplot) Same as the upper subplot but the behavior is depicted in the baseband ranging from the frequency 0 to $f_0 = 0 : 0078125$.

The frequency behavior of the filters $H_3(z)$ (designed in Section 3) with quantized and nonquantized coefficients using the droop compensator is contrasted to the frequency response of a classical third-order filter in Fig. 5. Notice that the droop compensator perfectly recovers the passband droop introduced by the decimation filters $H_3(z)$ since

$$\left[H_3(e^{j2\pi f})H_c(e^{j2\pi f})\right]\Big|_{f=0.0078125} \approx 1.$$

An effective architecture for implementing the proposed third-order filter with droop compensator is shown in Fig. 6. Notice that the compensator is moved at the lower rate after the decimator block.

Let us briefly compare the sample GCF filter to the techniques in [18] and [19]. As far as the computational complexity of the proposed droop compensator is concerned, we notice that $H_c(z)$ is multiplierless, and the terms A and B can be realized as shift registers. Fernandez Vazquez and Dolecek [19] addressed the design of droop compensators for GCFs employing maximally flat, least-square, and minimax criteria. We notice in passing that such criteria improve the passband droop introduced by GCFs to the same extent of the droop compensator in (17) but at the price of one real coefficient if the maximally flat and least-square criteria are adopted and two real coefficients if the minimax criterion is employed. In this respect, the droop compensator in (17) is, by far, more economical since no real coefficients are needed in the practical implementation.

In [18], the technique for droop compensation is based on the sharpening technique, which requires more complex structures than the simple droop compensator in (17).

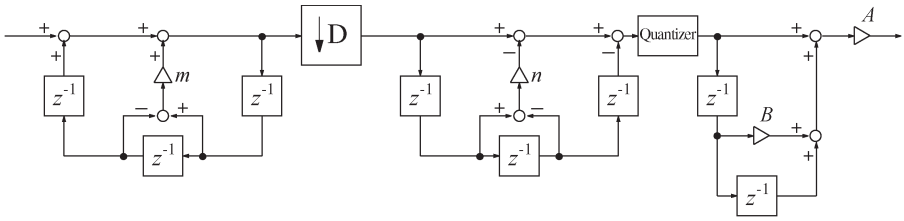

Fig. 6. Architecture of the decimation filter $H_3(z)$ with droop compensator. The coefficients noted in the figure are $A = -2^{-(r+1)}$ and $B = -(2^{r+2} + 2)$ specified in Table I.

V. Higher Order GCFs: Some Considerations

Higher order GCFs can be obtained using multiple instances of the basic cells

$$\frac{1 - z^{-D}}{1 - z^{-1}}, \quad \frac{1 - 2\cos(\alpha D)z^{-D} + z^{-2D}}{1 - 2\cos(\alpha)z^{-1} + z^{-2}}. \tag{18}$$

As an instance, a fourth-order GCF is identified by the following z-transfer function $H_4(z)$:

$$\frac{1 - 2\cos(\alpha_1 D)z^{-D} + z^{-2D}}{1 - 2\cos(\alpha_1)z^{-1} + z^{-2}} \frac{1 - 2\cos(\alpha_2 D)z^{-D} + z^{-2D}}{1 - 2\cos(\alpha_2)z^{-1} + z^{-2}}. \tag{19}$$

Using a similar reasoning, a fifth-order GCF is synthesized using three cells as follows:

$$H_5(z) = \frac{1 - z^{-D}}{1 - z^{-1}} \frac{1 - 2\cos(\alpha_1 D)z^{-D} + z^{-2D}}{1 - 2\cos(\alpha_1)z^{-1} + z^{-2}} \cdot \frac{1 - 2\cos(\alpha_2 D)z^{-D} + z^{-2D}}{1 - 2\cos(\alpha_2)z^{-1} + z^{-2}}. \tag{20}$$

The choice of the optimal α_1 and α_2 has been addressed in [8] (see also [22]) for different filter orders. Multiplierless implementations of these filters can be accomplished using the same technique presented in Sections II and III in order to represent the coefficients $2\cos(\alpha_1)$, $2\cos(\alpha_1 D)$, $2\cos(\alpha_2)$, and $2\cos(\alpha_2 D)$ as PO2 terms.

VI. Conclusion

This brief has focused on the design of recursive multiplierless GCFs by proposing an effective technique to jointly quantize the coefficients in the z-transfer function in such a way as to meet perfect pole–zero cancelation.

We have also proposed the use of a very efficient second-order droop compensator to recover the passband distortion introduced by this class of filters and briefly addressed the design of multiplierless higher order GCFs.

References

[1] S. R. Norsworthy, R. Schreier, and G. C. Temes, *Delta-Sigma Data Converters, Theory, Design, and Simulation*. Piscataway, NJ: IEEE Press, 1997.

[2] E. B. Hogenauer, "An economical class of digital filters for decimation and interpolation," *IEEE Trans. Acoust., Speech, Signal Process.*, vol. ASSP-29, no. 2, pp. 155–162, Apr. 1981.

[3] J. C. Candy, "Decimation for sigma delta modulation," *IEEE Trans. Commun.*, vol. COM-34, no. 1, pp. 72–76, Jan. 1986.

[4] P. P. Vaidyanathan, *Multirate Systems and Filter Banks*. Englewood Cliffs, NJ: Prentice-Hall, 1992.

[5] R. E. Crochiere and L. R. Rabiner, *Multirate Digital Signal Processing*. Englewood Cliffs, NJ: Prentice-Hall, 1983.

[6] F. Mintzer, "On half-band, third-band, and Nth-band FIR filters and their design," *IEEE Trans. Acoust., Speech, Signal Process.*, vol. ASSP-30, no. 5, pp. 734–738, Oct. 1982.

[7] F. Mintzer and B. Liu, "Aliasing error in the design of multirate filters," *IEEE Trans. Acoust., Speech, Signal Process.*, vol. ASSP-26, no. 1, pp. 76–88, Feb. 1978.

[8] M. Laddomada, "Generalized comb decimation filters for ΣΔ A/D converters: Analysis and design," *IEEE Trans. Circuits Syst. I, Reg. Papers*, vol. 54, no. 5, pp. 994–1005, May 2007.

[9] L. Lo Presti, "Efficient modified-sinc filters for sigma-delta A/D converters," *IEEE Trans. Circuits Syst. II, Analog Digit. Signal Process.*, vol. 47, no. 11, pp. 1204–1213, Nov. 2000.

[10] M. Laddomada, L. Lo Presti, M. Mondin, and C. Ricchiuto, "An efficient decimation sinc–filter design for software radio applications," in *Proc. IEEE SPAWC*, Mar. 20–23, 2001, pp. 337–339.

[11] L. Lo Presti and A. Akhdar, "Efficient antialiasing decimation filter for ΣΔ converters," in *Proc. ICECS*, Sep. 1998, vol. 1, pp. 367–370.

[12] Y. Gao, J. Tenhunen, and H. Tenhunen, "A fifth-order comb decimation filter for multi-standard transceiver applications," in *Proc. IEEE ISCAS*, May 2000, pp. III-89–III-92.

[13] H. Aboushady, Y. Dumonteix, M. Louërat, and H. Mehrez, "Efficient polyphase decomposition of comb decimation filters in ΣΔ analog-to-digital converters," *IEEE Trans. Circuits Syst. II, Analog Digit. Signal Process.*, vol. 48, no. 10, pp. 898–903, Oct. 2001.

[14] A. Y. Kwentus, Z. Jiang, and A. N. Willson, Jr., "Application of filter sharpening to cascaded integrator-comb decimation filters," *IEEE Trans. Signal Process.*, vol. 45, no. 2, pp. 457–467, Feb. 1997.

[15] G. J. Dolecek and S. K. Mitra, "A new two-stage sharpened comb decimator," *IEEE Trans. Circuits Syst. I, Reg. Papers*, vol. 52, no. 7, pp. 1414–1420, Jul. 2005.

[16] M. Laddomada, "Design of multistage decimation filters using cyclotomic polynomials: Optimization and design issues," *IEEE Trans. Circuits Syst. I, Reg. Papers*, vol. 55, no. 7, pp. 1977–1987, Aug. 2008.

[17] G. J. Dolecek and S. K. Mitra, "Simple method for compensation of CIC decimation filter," *Electron. Lett.*, vol. 44, no. 19, pp. 1162–1163, Sep. 2008.

[18] G. J. Dolecek and F. Harris, "Design of wideband compensator filter for a digital IF receiver," *Dig. Signal Process.*, vol. 19, no. 5, pp. 827–837, Sep. 2009.

[19] A. Fernandez Vazquez and G. J. Dolecek, "A general method to design GCF compensation filter," *IEEE Trans. Circuits Syst. II, Exp. Briefs*, vol. 56, no. 5, pp. 409–413, May 2009.

[20] M. Laddomada and M. Mondin, "Decimation schemes for ΣΔ A/D converters based on Kaiser and Hamming sharpened filters," *Proc. Inst. Elect. Eng.—Vis., Image Signal Process.*, vol. 151, no. 4, pp. 287–296, Aug. 2004.

[21] F. Daneshgaran and M. Laddomada, "A novel class of decimation filters for ΣΔ A/D converters," *Wireless Commun. Mobile Comput.*, vol. 2, no. 8, pp. 867–882, Dec. 2002.

[22] M. Laddomada, "Comb-based decimation filters for ΣΔ A/D converters: Novel schemes and comparisons," *IEEE Trans. Signal Process.*, vol. 55, pt. 1, no. 5, pp. 1769–1779, May 2007.

[23] I. S. Gradshteyn, I. M. Ryzhik, A. Jeffrey, and D. Zwillinger, *Table of Integrals, Series, and Products*. New York: Academic, 2000.

[24] H. G. Göckler, G. Evangelista, and A. Groth, "Minimal block processing approach to fractional sample rate conversion," *Signal Process.*, vol. 81, no. 4, pp. 673–691, Apr. 2001.